AUTONOMOUS VEHICLES

An autonomous excavator system for material loading tasks

Liangjun Zhang[1]*, Jinxin Zhao[1], Pinxin Long[2], Liyang Wang[1], Lingfeng Qian[2], Feixiang Lu[2], Xibin Song[2], Dinesh Manocha[3]

Excavators are widely used for material handling applications in unstructured environments, including mining and construction. Operating excavators in a real-world environment can be challenging due to extreme conditions—such as rock sliding, ground collapse, or excessive dust—and can result in fatalities and injuries. Here, we present an autonomous excavator system (AES) for material loading tasks. Our system can handle different environments and uses an architecture that combines perception and planning. We fuse multimodal perception sensors, including LiDAR and cameras, along with advanced image enhancement, material and texture classification, and object detection algorithms. We also present hierarchical task and motion planning algorithms that combine learning-based techniques with optimization-based methods and are tightly integrated with the perception modules and the controller modules. We have evaluated AES performance on compact and standard excavators in many complex indoor and outdoor scenarios corresponding to material loading into dump trucks, waste material handling, rock capturing, pile removal, and trenching tasks. We demonstrate that our architecture improves the efficiency and autonomously handles different scenarios. AES has been deployed for real-world operations for long periods and can operate robustly in challenging scenarios. AES achieves 24 hours per intervention, i.e., the system can continuously operate for 24 hours without any human intervention. Moreover, the amount of material handled by AES per hour is closely equivalent to an experienced human operator.

INTRODUCTION

Excavation is the process of moving earth, rock, or other materials with tools, explosives, or heavy equipment. It is frequently used in different applications corresponding to mining, exploration, environmental restoration, archaeological investigations, construction, and emergency rescue. Excavators are considered the most versatile heavy equipment and have a vast market. The size of the global market for excavators was US $44.12 billion in 2018 and is predicted to grow to US $63.14 billion by 2026 (*1*, *2*). In China, about 1.6 million excavators were in operation in 2018, and a total of 380,000 new excavators are projected to be sold in 2024 (*3*). However, excavating is recognized as one of the most hazardous operations (*4*, *5*) and results in a high number of injuries and deaths each year. In the United States, about 200 casualties occur per year (*6*) from cave-in, ground collapse, or other excavation incidents (Fig. 1). The number of injuries and deaths would grow even larger with more excavators in use.

Currently, excavators are controlled by human operators that have undergone specific training (*4*). This prolonged training includes learning not only excavating maneuvering techniques but also safety regulations and standards. In addition to life-threatening incidents, human operators may have to operate excavators in extreme working conditions. For example, a mining site (Fig. 1, C to F) is usually located in a remote area or even in a desert, where conditions include heavy dust and extreme high or low temperatures. Moreover, the remote location and long distances from cities result in limited availability of on-site excavator operators. Hence, workers suffer from prolonged working hours and loads, which can result in higher fatigue and more injuries (*7*). Globally, the mining and construction workforce is facing aging issues and labor shortages for operating heavy equipment, including excavators (*8*). One solution is to develop autonomous excavators that can operate in challenging and hazardous conditions without any human operator. An uncrewed excavation system may substantially reduce the number of casualties or injuries during excavation operations. Moreover, such an excavator could conduct tedious and repetitive tasks for extended hours, thereby increasing the overall throughput.

Efficiency, robustness, and generalizability are the three essential requirements in terms of designing an autonomous excavator (*9*, *10*). In other words, the autonomous excavator should operate without human intervention while performing a human-equivalent workload. In addition, the resulting excavator system should be capable of perceiving the surrounding environment to monitor the target material status and detect impurities and obstacles under extreme conditions. The system should generate feasible motions while avoiding any collision with the obstacles. The desired system should also handle many types of environments and materials and operate during different weather conditions.

Current excavators can be classified on the basis of their sizes. A compact excavator typically weighs less than 7 metric tons, a standard excavator weighs between 7 and 45 metric tons, and a large excavator weighs above 45 and, at most, 900 metric tons. Most excavators use hydraulic actuators, which allow excavators to perform many functions, including earth-moving and lifting and placing heavy objects. Ideally, we want to develop a general autonomous system architecture that can be applied to all these different types of excavators for various tasks. In terms of designing an autonomous excavator architecture that can operate robustly in real world scenarios, we address these challenges as follows:

1) The system needs to operate under an extensive range of environmental conditions that vary by the terrain types, weather, and lighting conditions. It is necessary that the perception module,

[1]Baidu USA, Sunnyvale, CA 94089, USA. [2]Baidu Research Institute, Beijing 100085, China. [3]University of Maryland, College Park, MD 20742, USA.
*Corresponding author. Email: liangjunzhang@baidu.com

Fig. 1. Challenges with respect to using excavators. (**A**) Land fall in excavation sites that cause excavator accidents, resulting in casualties or injuries of human operators. (**B**) An excavator that caught fire in an accident. (**C** to **F**) Excavators operate in extreme working conditions, such as excessive dust, severe vibration, high and low temperatures, or in remote areas. (**G**) Human fatigue impairs an excavator operator's ability to safely and effectively perform the job. (**H**) The mining and construction workforce is facing aging issues and labor shortages in terms of operating heavy equipment, such as excavators. Our AES system is designed to address these challenges and operate automatically without any human operator intervention in challenging scenarios.

which is responsible for understanding the surrounding environments, functions in different scenarios.

2) Excavators are frequently used to load a pile of material onto dump trucks. We refer to the material as the target material. Moreover, the shape of the target material pile changes after each loop of scooping and dumping the material. As a result, we need real-time techniques for online modeling of the shape and material type of the pile.

3) Scooping of the material has to be successful regardless of the type or characteristics of the material, which varies based on the density, hardness, or texture.

4) After scooping the material, the excavator has to successfully dump the material into a truck while avoiding any collisions with the truck, material pile, or other obstacles in the environment.

5) The location of the dump truck body area could vary considerably during the excavation. We need to develop robust online detection methods to determine the truck pose.

In light of these challenging excavating scenarios, we present a set of algorithms and a robust system architecture for our autonomous excavator system (AES). As shown in Fig. 2, our system consists of three main modules—perception, planning, and control—together with a hardware sensors layer and a graphical user interface (GUI) application layer. The planning and control modules are driven by the perception results. Specifically, we mount LiDAR (light detection and ranging), cameras, and a real-time kinematic (RTK) positioning device on the excavator and use a multimodal sensor-fusion approach to perceive the surroundings and the attributes of the target objects, including source material piles, dump trucks, dumping area, impurities, and obstacles. Our perception pipeline follows the "coarse-to-fine" manner, which not only can reduce the overall runtime but also can improve the system performance, enabling prolonged automatic operations without human operator assistance. Furthermore, to reduce the influence of dust, which heavily affects the recognition of obstacles in the excavation operation, we apply a state-of-the-art dedusting neural network to effectively generate cleaner images from dusty images.

On the basis of the perception results, we design a hierarchical planning module composed of a task-level planning layer and a motion planning layer for both excavator arm and base movement. Our planning approach combines the strength of inverse reinforcement learning (IRL) and data-driven imitation learning (IL) with the efficiency of optimization-based methods. The excavation target selection in task-level planning tries to learn the motion corresponding to excavation strategy, e.g., the next scooping position, from human operator demonstration. The motion generation layer uncovers the motion pattern of human-operated excavation movements. We integrate this motion pattern with a stochastic optimization-based algorithm for trajectory generation for scooping and dumping motions. Additional obstacle avoidance constraints corresponding to trucks or buildings are also added to our optimization formulation. To plan the movement of the excavator base and the arm, we decompose the overall task into a sequence of excavation subtasks based on the reachability map of the excavator arm. Our planning algorithm assumes that the excavator base remains stationary for each excavation subtask. Between different subtasks, we use a search-based motion planner to generate feasible paths for the excavator's base.

Excavator motion control can be challenging because the hydraulic excavator is a complex nonlinear system with a large time delay and is subject to large disturbances during excavation. We use a hierarchical motion controller, which consists of a high-level joint position controller for each arm, a bucket-end effector following the controller, an excavator base track controller, and low-level machine-specific look-up tables, which map the joint velocity to the hydraulic valve command. Our controller design can adapt to different excavators and works well in our scenarios.

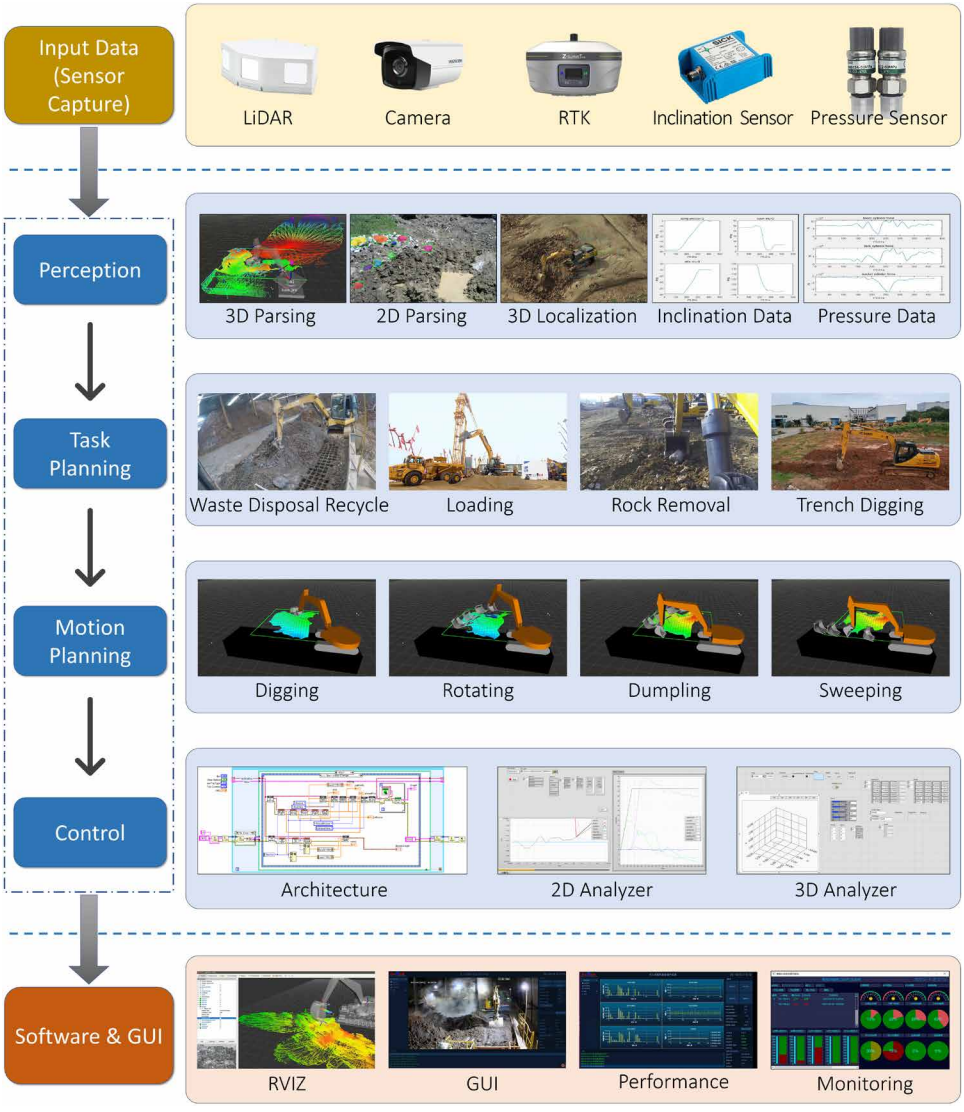

Fig. 2. Overview of our AES. LiDAR and camera sensor data are captured. The perception module parses the 3D point-cloud and image data for the surrounding areas by checking for target material, dump truck, impurities of the material, material and textures. This information is passed into the task planning module to determine the job plan. The motion planning module generates a feasible trajectory based on excavation constraints. The controller follows the planned trajectory. Software and GUI are developed for system integration, deployment, and daily use by end users.

Our modular architecture design (Fig. 2) allows AES to be generalized to various compact, standard, and large excavators. This generalization is achieved by parameterizing the size of the excavators within the system's perception, planning, and control modules and decoupling the high-level motion generation and the low-level hydraulic valve control. Our AES has been tested on 6– and 7.5–metric ton compact excavators, 33.5–metric ton standard excavators, and 49–metric ton large excavators. The AES has been extensively evaluated in real-world scenarios and designated test facilities.

The details of various scenarios are described in Table 1. During the material loading excavation operation, the autonomous excavator performs the normal scooping motion and dumps the target material. Simultaneously, the autonomous system handles terrain manipulation, obstacle avoidance, and any water in the scene. In this context, terrain manipulation indicates that objects such as rocks or impurities could appear in the working area and block the normal excavation motion. In these scenarios, the excavator needs to lift and remove such objects to load the target material successfully. Obstacle avoidance is performed during the loading operation. It ensures that the excavator will not collide with any dump trucks, or the material pile after each scooping, and any nontargeted materials. We highlight these tasks being performed in our test scenarios (Fig. 3).

We have deployed AES in real-world scenarios, where two excavators automatically operated in recycling pipelines and handled hazardous industrial solid waste material produced by various industrial activities. We demonstrate that our system can be seamlessly integrated within the pipelines for loading and dumping industrial waste—such as gypsum, dirt, gravel, or chemicals—that is hazardous for human operators. We have extensively tested AES in such scenarios, and our system can achieve 24 hours of continuous operation in an indoor setting (see Fig. 4). We further compare our autonomous excavator system's efficiency with skillful human operators. In terms of overall throughput, AES efficiency is closely equivalent to that of an expert human operator.

Overall, the contributions of our work include the following:

1) A perception-centered architecture that enables the excavator to handle various challenging scenarios. This architecture improves the system efficiency, robustness, and generalizability.

2) A hierarchical planning and control module that combines the strengths of the learning-based data-driven method, the optimization-based algorithms, and the joint position and bucket-end-effector motion-tracking schemes.

3) An AES, which can continuously operate for more than 24 hours without human assistance. We have thoroughly tested the performance of AES on multiple real-world scenarios. In addition, our system has been integrated with multiple types of excavators and tested by heavy equipment manufacturers.

Previous work

Several autonomous excavator–related algorithms and prototype systems have been developed and tested. The early development of autonomous excavator dates back to the 1990s. In (*11*), an autonomous loading system (ALS) was presented. An ALS relies on a laser scan for perception to detect a single truck model, and the system handles a single type of uniform soil without any impurity or change

Table 1. Scenario setups. We evaluated the performance of AES on 10 different scenarios. Our system operates robustly in these scenarios. The second column of the table lists each scenario's name, and the other columns indicate whether the corresponding functions need to be conducted in the related scenario. Loading, dumping, rock removal, obstacle avoidance, water recognition, and base movement are common functions that AES currently considers for performing successful material loading tasks.

	Scenario	Loading and dumping	Rock removal	Obstacle avoidance	Handling water	Base movement
1	Material loading and dumping	✓	–	–	–	–
2	Rock removal	✓	✓	–	–	–
3	Obstacle avoidance	✓	–	✓	–	–
4	Loading with rain	✓	–	–	✓	–
5	Rock removal with obstacle avoidance	✓	✓	✓	–	–
6	Rock removal with water handling	✓	✓	–	✓	–
7	Obstacle avoidance with water handling	✓	–	✓	✓	–
8	Full stack scenario	✓	✓	✓	✓	–
9	Trenching	✓	–	–	–	✓
10	Big pile removal	✓	–	–	–	✓

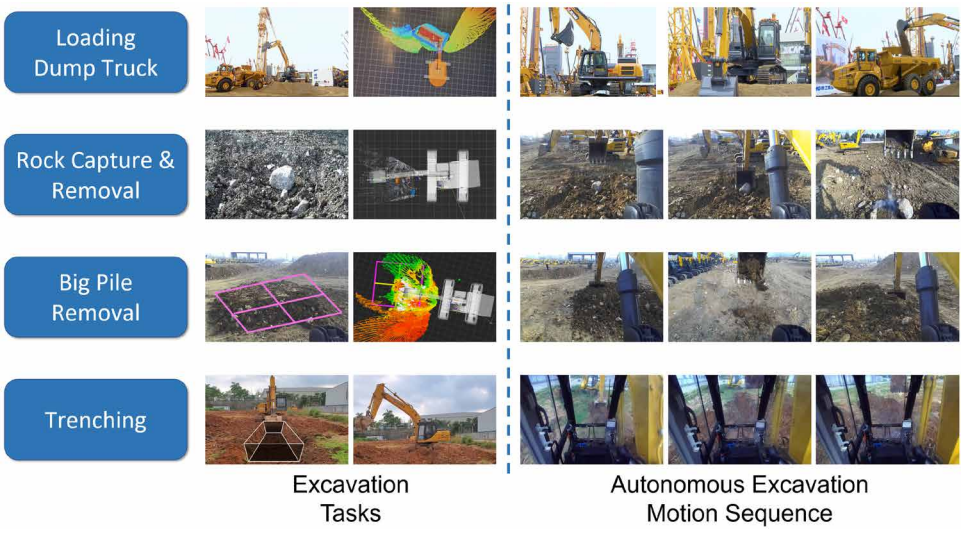

Fig. 3. AES validation scenarios. We have developed AES and validated on various scenarios, including material loading to dump truck, isolated rock capturing and removal, big pile removal, and trenching. We illustrate each high-level task and highlight various configurations of our autonomous excavator for these real-world scenarios.

of texture. After the ALS, other system architectures for autonomous excavators have been proposed (*12*–*14*). For example, Kim and Russell (*12*) introduced a conceptual framework of a semi-autonomous earthwork system while human intervention is minimized. Moreover, many heavy equipment manufacturers such as Caterpillar are also making an effort to bring autonomy into the construction industry (*15*). Currently, they focus more on semi-automatic remote control techniques.

Along with the overall system integration, numerous methods and algorithms have been investigated for individual modules, especially planning and perception. Singh and Cannon (*16*) introduced a classic planner architecture for earth-moving tasks. This architecture divides the planner into a coarse planner and a refined planner, which are responsible for planning the scooping region and excavation motion. Our autonomous excavator planning module uses a similar pipeline but improves each layer with improved planning algorithms for real-world deployment.

For the coarse task planner, Seo *et al.* (*13*) focused on the design of an excavation motion sequencing problem to arrange an efficient schedule for the excavation task based on coverage planning rules. A control method was discussed in (*17*) to improve the motion trajectory tracking accuracy. An optimization-based method for excavator trajectory generation was presented in (*18*). Recently, an advanced planning and control algorithm (*19*) was proposed to generate digging motions for excavation. This method constrains the interaction force during the digging motion, providing in-depth insights into autonomous excavator motion planning and control.

Recent advances in computer vision, deep learning, and LiDAR sensors can be used to improve the perception capabilities of excavators. Robust and accurate perception results are crucial for an autonomous excavator to understand the surroundings and targets with fine granularity and then perform appropriate planning operations. A rock detection and segmentation method based on the images of Mars terrain was discussed in (*20*). Moreover, Shariati *et al.* (*21*) describes a safety check perception module to detect excavator bucket

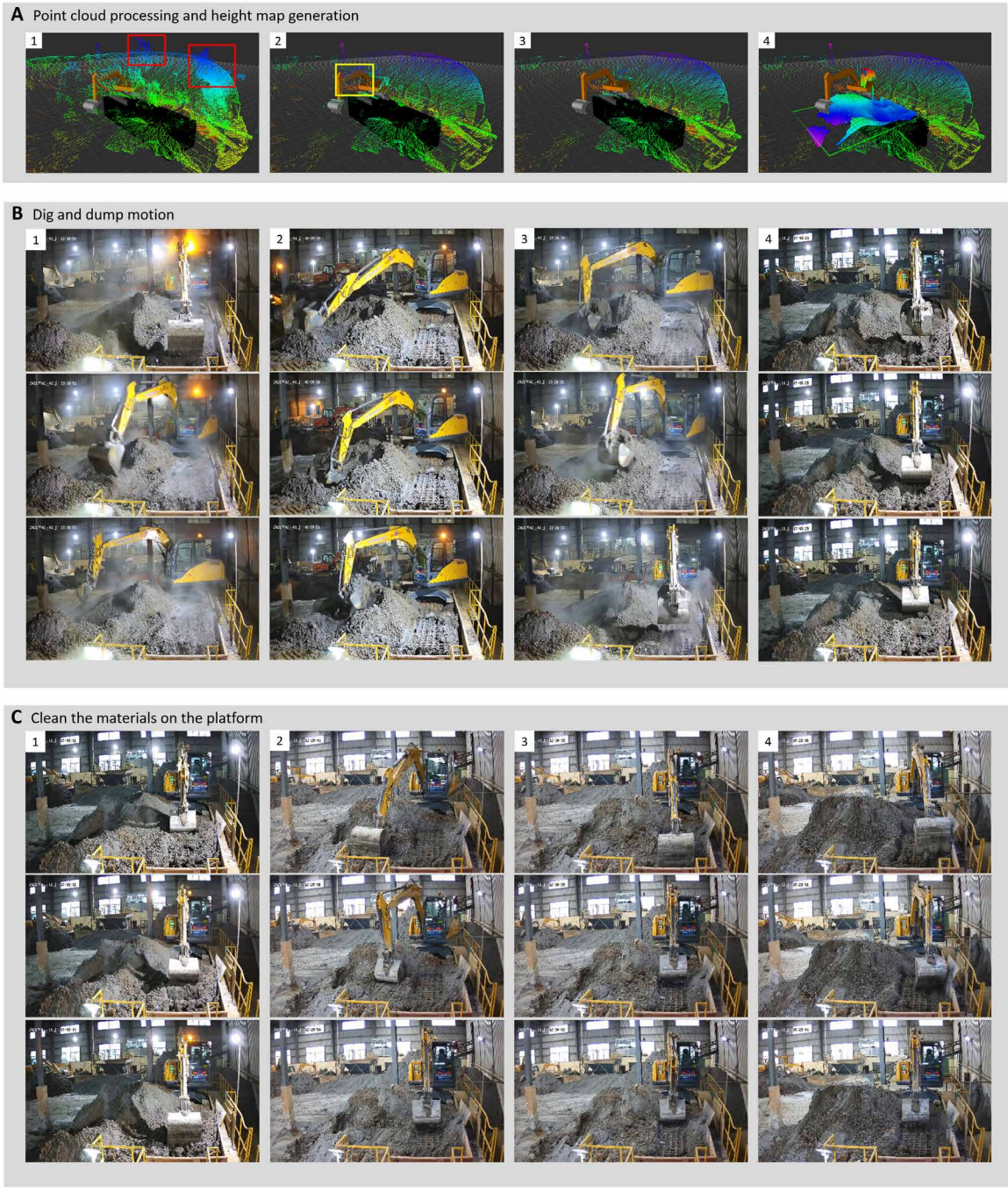

Fig. 4. Robust and nonstop operation of AES in a real-world waste disposal scenario. (**A**) (1) The raw LiDAR point cloud is first filtered by the intensity and noisy filters to eliminate the impact of vapor (red boxes). (2) Next, a self-filter is used to remove points from the excavator itself (yellow box). (3 and 4) Last, the filtered point cloud is used to generate the height map of working area. (**B**) The digging and dumping operation at different time of the day, including (1) the swing motion of the excavator arm to the digging area, (2) digging motion, (3) swing to dumping area, and (4) dumping on the platform. (**C**) The compliant sweeping motions are performed to clean the materials on the platform, which consist of (1) sweeping the materials after dumping, (2) cleaning the right part of the platform, (3) cleaning the forepart of the dumping area, and (4) cleaning the left part of the platform.

abnormalities. In summary, existing state-of-the-art methods focus on single perception functionality. However, our goal is to deliver a robust perception-centered architecture that satisfies overall fully automatic excavation perception requirements.

Although some of these prototype systems can perform specific tasks under restricted conditions, rarely have any autonomous excavators been deployed in real-world scenarios. Our AES is an uncrewed excavator system that has been deployed in real-world

Excavator Model		49.0-ton Large		33.5-ton Standard		7.5-ton Compact	
Excavator Arm Key Dimensions	Boom Length (m)	6.67		6.15		3.72	
	Stick Length (m)	2.91		2.91		1.62	
	Bucket Length (m)	1.92		1.69		0.89	
	Bucket Width (m)	1.52		1.41		0.94	
	Bucket Volume (m^3)	2.90		2.00		0.40	
Material Loading Average Time Per Loop (Human v.s. AES)	Move to Dig Area (s)	6.8	8.0	5.7	7.4	4.4	3.9
	Dig (s)	5.8	7.4	5.4	6.7	2.3	5.5
	Move to Dump Area (s)	9.0	10.1	8.1	9.0	4.3	3.8
	Dump (s)	2.1	2.3	2.1	2.3	4.4	7.1
	Sweep (s)	-	-	-	-	2.5	3.3
	Total Loop Time (s)	23.7	27.8	21.3	25.4	17.9	23.6
Efficiency Analysis (Human v.s. AES)	Bucket Full Rate (%)	90	95	92	95	115	110
	Excavation Efficiency (m^3/h)	396.5	356.8	311.0	269.3	67.4	67.1
	AES v.s. Human Effiency	90.0%		86.6%		99.6%	

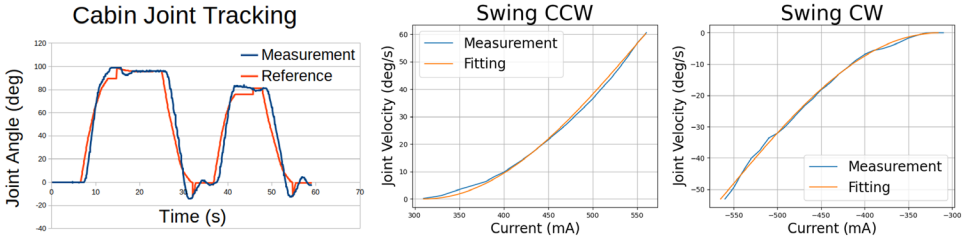

Fig. 5. AES performance. (**Top**) Efficiency comparison between AES and human operators in terms of average time used for each loading loop and bucket fill rate. Ranging from large to compact excavators, AES is as efficient as a human operator on average in terms of the amount of material loading per hour. (**Bottom**) The plot on the left highlights the controller tracking performance for the excavator swing and the controller follows the reference joint trajectory closely. The other two plots highlight the mapping between swing joint velocity and the current for hydraulic valve command.

scenarios and used by manufacturers of heavy machinery and the construction industry. We developed a perception system that fuses three-dimensional (3D) LiDAR and camera outputs to perceive the 3D environment. The combination of LiDAR and cameras helps detect both the type and location of the targets. Our excavator planning module takes advantage of the advanced data-driven methods and stochastic optimization for motion generation. Our planning module is integrated and thoroughly tested with our perception module. The combination results in a robust and efficient autonomous excavator that can operate for long hours without human intervention.

RESULTS

Our autonomous excavation system has been evaluated under multiple controlled, real-world testing scenarios. To thoroughly test the system capability, we set up scenarios in a closed test field, mimicking common real-world use cases for an excavator. On the basis of the successful test results in these scenarios, we also evaluated the efficiency and robustness of the system in one of our deployment sites, a waste disposal factory. We show that our AES can continuously operate for 24 hours without any human intervention. In terms of efficiency or throughput, AES is close to a human operator, as measured by the amount of material handled during the same amount of time.

System verification using different excavation scenarios

Scenario 1: Material loading and dumping

This is a basic test scenario, where the material is free of impurities, and there are no obstacles or water in the scene. This scenario helps us to evaluate terrain modeling perception and basic excavation motion generation for loading and dumping the target material into a dump truck, as shown in Fig. 3 (loading dump truck). We performed a comparison experiment to investigate the excavator efficiency between our autonomous system and human operators in this scenario. In terms of the average time used for loading and dumping task, our autonomous system is about 85 to 90% as efficient as a human operator on standard- and large-size excavators. Specifically, we divide each loading and dumping loop into four phases, including "dig," "swing to dump area," "dump," and "swing back." Specifically, dig indicates loading the excavator bucket with target material; swing to dump indicates swinging the excavator bucket to the dumping area, such as the truck region; dump means unloading the material from the bucket to the dumping area, such as the truck bed; and swing back means swinging the bucket back to face the working area. In Fig. 5, we show the performance for each period and bucket-filling rate in average, which corresponds to the percentage of the bucket that is loaded during each operation.

Scenario 2: Rock removal

In this scenario [Fig. 3 (rock removal)], the excavator needs to lift stones or rocks that block its working area to enable the excavation task. The scenario is designed to extensively test the stone identification module and perform appropriate task/motion planning. The stone identification perception module outputs the 3D bounding boxes for the target stone or rocks. On the basis of the perception results, the motion planning module generates a feasible trajectory for the excavator arm motion to capture the object.

Scenario 3: Obstacle avoidance

In this scenario, we detect the obstacles and then optimize a collision-free trajectory. Specifically, the obstacles correspond to the loading trucks, surrounding buildings, impurities, and piled materials. The reason to avoid impurities is that impenetrable impurities can jam or block the excavator's arm motion. The excavator arm should avoid any contact with the pile after filling up the bucket before dumping the material into the truck.

Scenario 4: Loading in rain

In many circumstances, an excavator needs to operate in the rain. It is highly possible that a puddle would appear around the working zone. To avoid scooping into the water, AES is capable of identifying the area filled with water. On the basis of these working conditions, we design a test scenario and verify the performance of our system.

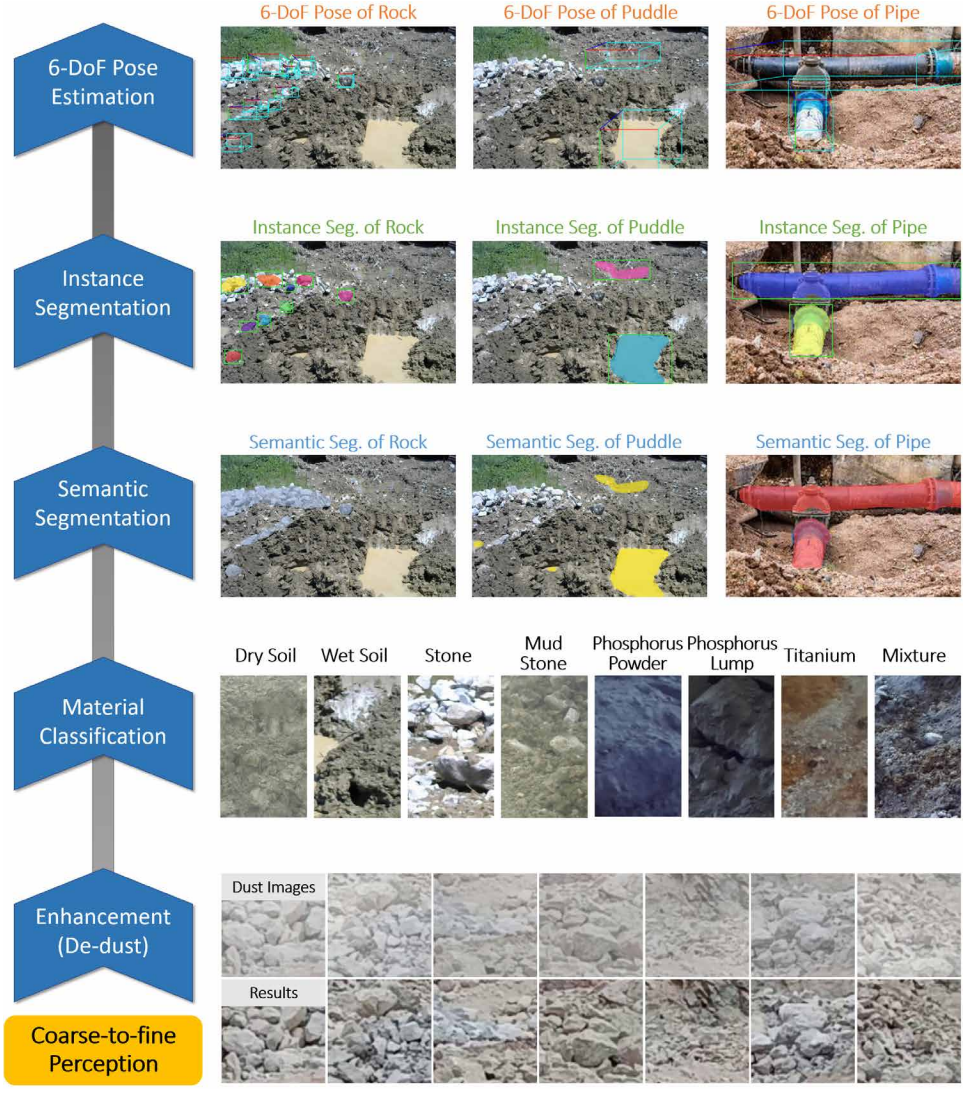

Fig. 6. Our coarse-to-fine perception pipeline in AES. Our perception module consists of image enhancement for dedusting, material textures classification, object and instance segmentation, and object 3D pose and shape detection. By using a multimodal LiDAR/camera sensor-fusion approach, our system can perceive the surroundings and the attributes of the target objects. The coarse-to-fine architecture not only can reduce the overall runtime but also can improve the perception performance.

Scenario 5: Combined scenario of rock removal with obstacle avoidance

This test scenario is closer to a realistic excavation scenario, combining scenarios 2 and 3. Our perception module is designed to label the blocking objects and segment the obstacles for a robust mining operation. Our task planner first decides whether to remove the blocking objects, and then the motion planner module generates the collision-free trajectory of the arm.

Scenario 6: Combined scenario of rock removal with water handling

When excavation happens during wet weather, the successful detection of both water and rocks is necessary. We therefore set up a new scenario that is a combination of scenarios 2 and 4. In this case, the perception module reliably identifies the blocking objects and segments the water area.

Scenario 7: Combined scenario of obstacle avoidance with water handling

To segment the obstacles and the water area, our perception module takes advantage of the semantic segmentation method. We verify these segmentation capabilities of the AES perception module during rainy days in scenarios with obstacles and impurities in the scene.

Scenario 8: Full-stack excavation scenario

This is a challenging but realistic excavation scenario, where different features and capabilities are combined. In this scenario, AES has to decide between scooping the material and removing the stone while avoiding any obstacles and water area. We can use this scenario to evaluate the robust capabilities of our perception, planning, and control modules.

Scenario 9: Trenching scenario

In this scenario, the excavator needs to repeat the steps corresponding to multiple digging and dumping operations and moving its base backward to dig a trench. The scenario is designed to evaluate AES in terms of moving the excavator base. This includes RTK-based base localization, perception of the shape of the trench using 3D point clouds captured using a LiDAR, planning and control for excavator base movement, and overall task planning for trenching. Figure 3 (trenching) shows the task and motion sequence generated by AES for the trenching scenario.

Scenario 10: Big soil pile removal scenario

This scenario is designed to test the capability of AES in terms of task planning and base movement. For a large pile of soil, the excavator is not able to remove all of the material using its arm movement without changing its base position. Our approach divides the entire work area into multiple task zones. The excavator needs to move different locations corresponding to each task zone and performs excavation operation for each task zone. Figure 3 (big pile removal) shows the scenario of a 7-m by 7-m pile, which is divided into four 3.5-m by 3.5-m square-shaped task zones (as shown in the leftmost image). The excavator moves around the pile to remove the soil within each square.

AES deployment for real-world scenario

For the waste disposal and recycling application, the excavator is assigned to load industrial waste material into a designated area. Afterward, the material is transferred and recycled. The material may consist of excessive dust, which is toxic to human beings. The material pile is not stable and could collapse, which is another threat

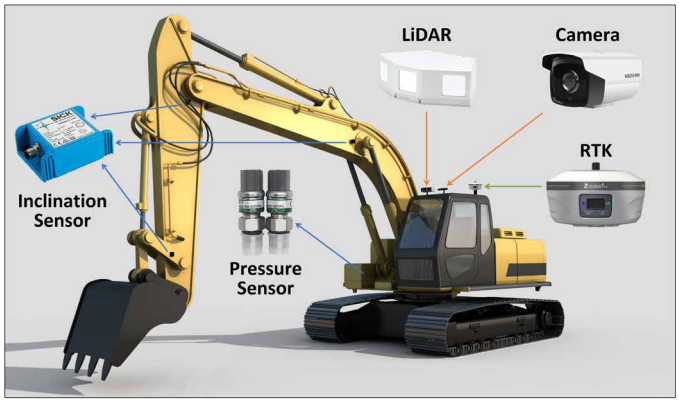

Fig. 7. Hardware sensors used in AES. Our AES is equipped with state-of-the-art sensors. We calibrated LiDAR and camera sensors and fused multimodal sensor data so that we can achieve reliable perception of the surrounding environment.

to human operators. The pipeline of the waste recycling is shown in Fig. 4. The speed of material loading by the excavator has to coordinate with the belt conveyor's speed and material processing rate. Hence, there is a high-efficiency requirement for our autonomous excavator. In addition to satisfying the efficiency requirement, our AES can handle both dry and wet materials. AES can also function at night. In this scenario, AES can operate a whole 24-hour day without any human intervention. The amount of the handled material is as much as 67.1 m^3/hour for the 7.5 ton of excavator, which is closely equivalent to a human operator's performance. Furthermore, AES performs consistently over time, whereas the performance of human operators may vary.

DISCUSSION

Our newly designed AES has been extensively tested for robustness and efficiency. Our AES is put into deployment for prolonged operations. It removes human operators from hazardous conditions in the waste disposal application and achieves 24 hours per intervention (HPI).

Compared with the existing uncrewed excavator system, our overall architecture largely relies on the perception module to perform fine-grained 2D/3D understanding of the surroundings and the target objects. Thus, the overall performance of our approach is mostly governed by the accuracy of perception algorithms and sensor hardware. In heavy machinery applications, the reliability of our sensor hardware plays an important role to ensure the robustness of AES. The recent developments in terms of better LiDAR and camera sensors and advanced computer vision algorithms can further improve our perception performance. We have not considered scenarios where snow or ice may be present. Such scenarios introduce many challenges not only for the perception module but also for the planning and control modules. As part of future work, we propose to evaluate and extend the capabilities of AES to handle more challenging weather and illumination conditions.

MATERIALS AND METHODS

Software architecture

There are four software modules in our system. The perception module was designed for sensing various obstacles, modeling the terrain, classifying the material, and locating the dump truck. On the basis of the perception results, the planning module optimizes the motion trajectories for the excavator arms and base. Then, the control module transfers the planning results to the hardware control commands, which are sent to the excavator to track the desired motion. On top of those modules, an application layer of the software is developed for different applications.

All modules ran simultaneously as nodes under the Robot Operating System (*22*) framework. In this section, we provide more details on the perception and planning modules, which are the key components that enable our system to be deployed in real-world scenarios. The overall architecture of AES is shown in Fig. 2.

Perception

Our perception module focuses on parsing and understanding the surroundings and identifying the target objects in the unstructured working zones. To handle various challenging scenarios, we performed fine-grained 2D/3D perception, including the following:

1) Identifying the blocking obstacles that need to be removed;

2) Detecting the impenetrable portion of the material to avoid direct contact between it and the excavator's arm;

3) Recognizing the texture of the material and modeling the shape of the material pile to perform the loading operation; and

4) Enhancing the images through computer vision methods, such as dedusting, which aims to remove the influence of dust in image capturing, thus to improve the performance of obstacles identification and texture recognition.

To this end, our perception module adopted a coarse-to-fine approach to detect, segment, and parse the larger-sized objects, small-sized targets, and material textures. Our perception module exploits state-of-the art algorithms, such as semantic segmentation (*23*, *24*), instance segmentation (*25*), texture and material recognition (*26*), and dedusting (*27*). Taking a stone detection and segmentation task as an example, an image enhancement algorithm was first used; then, a texture and material recognition algorithm was exploited to identify the stone/puddle/pipe area from the whole image; a 2D detection and segmentation algorithm was used to segment these objects accurately; last, the 2D segmentation and LiDAR's depth information were combined for fitting the 3D bounding box to each detected obstacle.

Image enhancement: Dedusting

During the excavation operation, especially for handling stone and soil, dust often exists in the working area. The dust can considerably affect the recognition of obstacles, such as rocks and trucks. To solve this problem, we used a dedusting neural network to generate clean images from dusty input images. In particular, an encoding module that aims to extract the multiscale features and a decoding module that contains a multiscale boosted strategy (*27*) were used in the dedusting network. Besides, an attention strategy (*28*) was used to intensify the features of the decoding module, thus better dedusting results can be obtained. To effectively train the dedusting network, we collected a dust dataset from the real-world excavation environment. Our dataset consisted of 1000 dusty images captured from real world (with image resolutions of 256 pixels by 256 pixels) and corresponding ground truth clean images for training and additional 200 images for testing. The offline training period took 5 hours using one Nvidia P40 graphics processing unit (GPU). Figure 6 [Enhancement (Dedust)] shows the results generated using our dedusting method.

Material classification

The properties of the loading material, such as the density and hardness, could significantly affect the excavation motion. We used a visual texture classifier based on the red-green-blue (RGB) image inputs to predict the material type. In particular, to effectively train the texture classifier, we collected a texture dataset captured from two environments: wild environment and chemical wastes for recycling. The dataset contained eight classes: dry soil, wet soil, stone, and mud stone (wild environment) and phosphorus powder, phosphorus lump, titanium, and the mixture of titanium and phosphorus (chemical wastes). The dataset contained 7563 images, 6720 images for training, and 843 images for testing. We used the Deep Encoding Pooling Network (*26*) with an attention strategy for texture classification and achieved an accuracy of 100%. The offline training period took 1 hour using one Nvidia P40 GPU.

Semantic segmentation: Obstacles

Another difficulty that commonly happens during the excavation operation is avoiding collisions with obstacles. Such obstacles include material impurities, the loading truck, the material pile after the scooping operation, etc. When the material contains hard impurities, it will prevent further movement of the excavator's arms after direct contact. This is more likely to happen when the end tip or the excavator's bucket-end effector contacts such impurities. In this case, the human operator typically performs a reasonable choice in terms of excavation motion to avoid direct contact between the impurities and the end tip of the bucket. To identify such scenarios, we performed semantic segmentation as shown in Fig. 6.

Instance segmentation: Blocking objects

In many excavation scenarios, blocking objects indicate the large-sized rocks or accumulated undesirable material impurities that can usually cause the excavation motion's failure. Human operators can remove this kind of object after a certain amount of training. To robustly remain in autonomous operation without human assistance, AES needs to have an equivalent ability to detect these objects. This part shows the results corresponding to blocking obstacle detection, where the pose and size of an obstacle were obtained through the RGB camera and LiDAR sensor fusion. The information was fed to the planning module to compute the trajectory to perform the rock-removing movement task. We used the Mask R-CNN (*25*) algorithm to identify the blocking obstacles in the scene with RGB input. For training the Mask R-CNN model, the training dataset contained 4000 rock or stone instances. The training period took 2 hours using 4 Nvidia 1080 GPUs.

Six-DoF pose estimation: Dump trucks and blocking objects

To perform truck pose estimation, a template truck model with 3D point cloud representation was computed offline. This was performed by scanning the truck from multiple perspectives and recording the point clouds. Next, we segmented each point cloud that corresponds to the truck and composed the resulting point clouds to obtain a truck template. During online truck pose estimation, the truck template model was matched with the point cloud from the LiDAR scan using an iterative closest point–based algorithm. Last, we used the estimated truck pose to determine the bucket location for material dumping. For blocking objects, such as stone or pipe, we leveraged the sensor fusion between the 3D LiDAR point cloud and camera image for shape and pose estimation. On the basis of the 2D instance segmentation results, the camera and LiDAR's depth information were combined and used for fitting the 3D bounding box to each detected obstacle. An example of stone pose estimation is shown in Fig. 6 (pose estimation).

Planning

Our planning module is closely related to the perception module, as shown in Fig. 2. To handle the real-world material loading task, the planning module needs to explicitly account for the terrain shape and the positions of the obstacles. Our hierarchical planning module automatically selects the target of excavation based on the perception results. The detailed arm motion is generated on the basis of this target. Thus, the planning module is composed of a task planning algorithm and a motion generation algorithm. This combination allowed us to use a data-driven method with an optimization-based algorithm.

Excavation target selection

We propose a data-driven method for target selection module (*29*). This module aims to learn the routine of a human operator according to the terrain observation of the excavation working zone. In this application, the terrain observation was selected as the 2.5D grid–based height map of the working area. The predicted outputs are the location of the point of attack (POA) and bucket travel length, where POA represents the point at which the excavator bucket first contacts the material. The travel length means the distance the bucket travels before lifting the material. A neural network model was designed for the learning task and is described as

$$y = f_{\text{core}}(x), \theta = y^{\mathrm{T}} M, z_{\mathrm{x}} = f_{\text{lon}}(\theta),\ z_{\mathrm{y}} = f_{\text{lat}}(\theta),\ z_{\mathrm{l}} = f_{\mathrm{l}}(\theta)$$

where x is the observation; f_{core} is a function of convolutional layers; f_{lon}, f_{lat}, and f_{l} are multilayer perceptron with trainable parameters; M is a matrix with trainable elements; z_{x} and z_{y} are the longitudinal and lateral coordinates of the POA; and z_{l} is the length that the excavator bucket travels before lifting. Our resulting model follows the idea of neural programming interpreter (*30*).

Excavation motion generation

Our motion generation module outputs the trajectory in the excavator joint space based on the target selection module. For this computation, we used a data-driven method to represent the human-operated excavation movement pattern. The pattern was implemented into an optimization-based method for generating the motion trajectory.

We used IRL (*31*) algorithm to uncover the motion pattern. Given a trajectory τ, the cumulative cost $C(\tau)$ is defined as

$$C(\tau) = \mathbf{w}^T \boldsymbol{\Psi}(\tau)$$

where $\boldsymbol{\Psi}$ is a user-defined feature function vector and $\mathbf{w}$ is the weight vector associated with the feature vector.

Given multiple collected human-operated excavation motion trajectories, the target is to learn the feature weight vector $\mathbf{w}$, which can be obtained by solving a convex optimization problem

$$min_{\mathrm{w}} \sum_{\mathrm{i}=1}^{D} \log \sum_{k=1}^{K} e^{-\mathbf{w}^T(\boldsymbol{\Psi}_{i,k} - \boldsymbol{\Psi}_i^*)} + \lambda \|\mathbf{w}\|_1$$

where D is the number of demonstration trajectories and K is the number of sampling trajectories for each demonstration trajectory. $\boldsymbol{\Psi}_i^*$ is the cumulative feature vector for the demonstration trajectory i, i.e., $\boldsymbol{\Psi}_i^* = \sum_{j=1}^{N} \boldsymbol{\Psi}_i(j)$, where N is the number of sample points of

the trajectory. $\Psi_{i,k}$ is the cumulative feature vector for the sample trajectory k around demonstration i.

On the basis of the computed POA and bucket travel length, the start and end excavator arm configurations can be calculated using inverse kinematics. In particular, we defined the features, including the squared errors between the specific configuration and the end configuration, the square of the velocity and acceleration with respect to each joint, and the squared distance between the bucket end effector to the terrain surface. We performed this learning computation in an offline manner.

During the online motion generation, the feature weights and cost features are used within stochastic trajectory optimization for motion planning (*32*, *33*). In addition to the human motion pattern, the trajectory optimization framework allows us to account for static and dynamic obstacles in the scene. In real-world scenarios, there may be impenetrable impurities in the material, and our perception module can identify the locations of such impurities. Therefore, additional cost features related to these obstacles are added to the overall cost function.

Excavator base movement

In addition to excavator arm movements, planning the excavator base movement is important to perform material loading jobs. For example, to load a large pile of soil, the excavator may not be able to remove all of the soil without changing the position of its base. In our approach, we decoupled the planning for excavator base and arm movements. This approach works well because in real-world scenarios, the excavator alternates between moving the base to the desired position and the motion of its arm to perform excavation operation. In terms of excavator base movement planning, there are two main issues: selecting a sequence of desired base positions to perform the given subtasks and safely navigating to the selected target base positions on the uneven terrain and avoiding collisions with the obstacles.

Task planning. We developed a fast method for excavator task planning with base movement. Given a high-level task, such as loading a large pile of soil material, our method partitions the entire work area into multiple task zones. The main idea is to compute a partition so that the base remains stationary for each task zone, and the excavation of each task zone is performed by only using the arm movements. Here, we divided the work area on the basis of predefined workspace division rules while considering the arm reachability constraints, then computed the route for the excavator to move to cover all the generated task zones (*13*, *34*).

Excavator base motion planning. Once a task route was computed, we computed a feasible path for the base so that it can reach each desired base location along the route. A 3D point-cloud map of the workspace was computed by using LiDAR-based mapping methods (*35*). Using RTK and LiDAR, our excavator can localize its base position within the map. Furthermore, traversable regions in the map were computed on the basis of point-cloud height information and can be further improved by identifying potential obstacles (e.g., big rocks) and infeasible regions (e.g., pits) using learning algorithms (*36*). An elevation map with occupancy information of the environment was obtained. We used a search-based motion planning method (*37*) to compute the feasible path for the excavator base to move from the current location to the target location and used a model predictive control–based motion controller so that the excavator can follow the planned path closely. Last, the hydraulic valve commands are computed by the low-level controller and used to move the excavator base.

System hardware

In this application, the robot platform (Fig. 7) was a hydraulic excavator equipped with the drive-by-wire system. Currently, we have developed and tested multiple different sizes of excavators, including 6.5 and 7.5 ton of compact excavators, 33.5 ton of standard excavators, and 49 ton of large excavators. These excavation platforms offer enormous output power to conduct various excavation tasks successfully. The manufacturer provides a control interface through a controller area network (CAN) bus so that the entire unit can be controlled by software. To ensure safety, a fall-back human control mechanism was implemented in case of an emergency.

To sense the excavator locations and motions, multiple sensors were installed. We used a Huace RTK positioning device for providing the location of the excavator. SICK and Honeywell inclinometers were used for measuring the angles of different joints of the excavator. During the hardware tests, such sensors have shown relatively accurate readings amid the excessive hardware vibrations. A combination of Livox mid-100 LiDAR sensors and RGB cameras collected the environmental information for the perception module to fuse, process, and analyze to understand the surroundings. One Intel i7 computer with Nvidia GPU, running Linux system, hosted the perception, planning, and control software modules. An industrial control board based on an STM32F407 arm microcontroller was used for low-level communication between the computing unit and the excavator through CAN interface.

Safety features

In deploying the AES to the real world, safety is always the most critical consideration. We designed two strategies to guarantee the safety of AES, including the offline predefined safety operation region for the excavator region in the map, and the online object detection and avoidance feature. The predefined safety region is specified by the user to preclude the area in the map of the environment. Our AES excavator, equipped with RTK and joint sensors, can measure the position of each link of the excavator arm and the position of its base so that any part of the excavator can be prevented from entering the specified safety region. Besides, our AES was equipped with state-of-the-art camera-based object detection software. Therefore, it can detect unexpected humans or animals in the excavator work space and stop any movement.

Limitations and challenges

Our current system has some limitations, including the limitations in the perception, planning, and control modules. Further, some of the errors get compounded in terms of the overall performance as these modules are integrated.

Perception

AES currently relies on perception sensors such as LiDAR and cameras for sensing the environments and deep-learning techniques for further modeling the target material and generating a representation. The shape and the appearance of the material/terrain were used to determine which parts of the desired materials are scooped and loaded. To extend AES to work in more diverse environments, the overall system needs to have a holistic understanding of the physical environments, which means being able to sense or model the material properties such as density, damping, stiffness, viscosity, or fluidity; infer the partially visible objects (e.g., partially buried pipes or occluded rocks); and understand and reason the semantic relationship between the objects within the scenes. For instance,

our current perception system detects ground water as obstacles to avoid, whereas a holistic understanding of the scene, e.g., the flow of the ground water, is often required to effectively manage the water during the excavation.

Furthermore, we used deep-learning techniques in our perception module, including material semantic segmentation, texture classification, object detection, and dedusting. As a consequence, the performance of the perception module relies on the quality of the training data, and it is difficult to provide guarantees on its robustness in all situations. For example, any objects encountered during deployment inference may not be similar with the training data. Besides, our current texture classification method can handle multiple types of materials, as shown in Fig. 6. If our AES encounters a new type of object or material (i.e., shape or texture) during deployment, then we need to retrain the system accordingly. The perception errors reduce when the size and variety of the training database improves. The perception system also needs to work in extreme conditions such as heavy dust, rain, wind, or snow. The initial results on dedusting are promising, although we need to test and extend this capability for all kind of scenarios.

Planning and control

The variety of the excavation tasks and terrain types, along with perception errors and uncertainty of the environment deformation, creates additional challenges for excavator motion and job planning. In our current work, we mainly deal with soil excavation and isolated rock removal. However, handling general terrains or rock excavation can be more challenging because of excessively large or unpredictable resistive force during the excavation. Furthermore, a human operator typically senses the material properties—such as damping, stiffness, viscosity, etc.—using visual and force feedback and adjusts the excavation motion and control strategy accordingly. Our current system mainly relies on prior knowledge about a limited set of predefined materials for generating suitable excavator arm motion and control commands, and force feedback has not been fully exploited. Therefore, the system still needs to be generalized so that it can be automatically adapted to different terrain types during the excavation task. In addition to arm motion generation, generating a safe and efficient excavation job plan, especially involving both base and arm movements, needs to be developed for challenging scenarios. For instance, AES operates only in the predefined safety region to avoid unsafe operations. Furthermore, base path planning and arm motion generations can be highly coupled, although they are not performed simultaneously. The end state of the base movement affects the arm motions for scooping the soil, whereas the new terrain generated from the scooping arm motion needs to be used to compute the safe region for excavator base movement.

System integration

Although our AES has demonstrated success in many material loading tasks, developing an integrated autonomous system and deploying it into all kind of real-world scenarios can be challenging, especially given that the system involves software and hardware level integration. During our evaluations, we observed noisy sensor readings or hardware sensors failures. For instance, the inclination meter sensor may not update or send abnormal readings. Such issues were resolved by using more robust hardware components. Through multiple iterations and developments, the reliability of hardware components required for autonomous systems was improved.

In terms of the overall cycle for AES development and deployment, the system integration and validation are the most time- and resource-consuming component. This is because fulfilling the requirements for any safe autonomous system requires intensive testing (*38*). To improve the overall development and validation efficiency, we have developed systematic validation methodologies for different level testing, including simulation-based validation of every individual software module, validating using real-world recorded data, and hardware-in-loop validation using real excavators. We will continue optimizing our validation methodologies and improve the efficiency of integration and validation so that more advanced autonomous features can be developed, validated, and deployed for real-world complex and hazardous scenarios.

SUPPLEMENTARY MATERIALS

robotics.sciencemag.org/cgi/content/full/6/55/eabc3164/DC1
Figs. S1 to S3
Movie S1

REFERENCES AND NOTES

1. Fortune Business Insights, Excavators market size, share and industry analysis by type (mini/compact excavator, crawler excavator, wheeled excavator, other excavator), by end-use industry (construction, forestry agriculture, mining, others) and regional forecast 2019–2026 (2019); www.fortunebusinessinsights.com/industry-reports/excavators-market-100861.
2. Grand View Research, Excavator market size, share trends analysis report by product (crawler, wheeled, mini/compact), by application (construction), by region, competitive landscape, and segment forecasts, 2018–2025 (2018); www.grandviewresearch.com/industry-analysis/excavators-market.
3. IndustryResearch, Global Excavator Market Report (2020);https://industryresearch.co/-global-excavator-market-15473051.
4. S. Afanuh, M. Gillen, T. Lentz, Preventing worker deaths from trench cave-ins;https://cdc.gov/niosh/docs/wp-solutions/2011-208/pdfs/2011-208.pdf?id=10.26616/NIOSHPUB2011208.
5. Occupational Safety and Health Administration, Excavation: Hazard recognition in trenching and shoring. (OSHA technical manual, 1999).
6. J. Lew, D. Abraham, R. Wirahadikusumah, J. Irizarry, C. Arboleda, Excavation and trenching safety: Existing standards and challenges, in *2002 Proceedings of Triennial Conference CIH WO99* (2002).
7. T. Bauerle, Z. Dugdale, G. Poplin, Mineworker fatigue: A review of what we know and future decisions. *Min. Eng.* **70**, 33 (2018).
8. Komatsu Inc., Komatsu Report 2020 (smart construction), *Tech. rep.* (2020). https://home.komatsu/en/ir/library/annual/pdf/KMTKR20EPrint.pdf[accessed January 2021].
9. S. Dadhich, U. Bodin, U. Andersson, Key challenges in automation of earth-moving machines. *Autom. Constr.* **68**, 212–222 (2016).
10. A. Hemami, F. Hassani, An overview of autonomous loading of bulk material, in *26th International Symposium on Automation and Robotics in Construction* (ISARC, 2009), pp. 405–411.
11. A. Stentz, J. Bares, S. Singh, P. Rowe, A robotic excavator for autonomous truck loading. *Auton. Robots* **7**, 175–186 (1999).
12. S.-K. Kim, J. S. Russell, Framework for an intelligent earthwork system: Part I. system architecture. *Autom. Constr.* **12**, 1–13 (2003).
13. J. Seo, S. Lee, J. Kim, S.-K. Kim, Task planner design for an automated excavation system. *Autom. Constr.* **20**, 954–966 (2011).
14. D. A. Bradley, D. W. Seward, The development, control and operation of an autonomous robotic excavator. *J. Intell. Robot. Syst.* **21**, 73–97 (1998).
15. Caterpillar Inc., Making jobsites safer, more efficient and more productive, *Tech. rep.*; https://cat.com/en GB/campaigns/event/bauma2019/innovation/autonomy.html [accessed January 2021].
16. S. Singh, H. Cannon, Multi-resolution planning for earth moving, in *Proceedings of the 1998 IEEE International Conference on Robotics and Automation* (IEEE, 1998), vol. 1, pp. 121–126.
17. P. H. Chang, S.-J. Lee, A straight-line motion tracking control of hydraulic excavator system. *Mechatronics* **12**, 119–138 (2002).
18. Y. Yang, P. Long, X. Song, J. Pan, L. Zhang, Optimization-based framework for excavation trajectory generation. *IEEE Robot. Autom. Lett.* **6**, 1479–1486 (2021).
19. D. Jud, G. Hottiger, P. Leemann, M. Hutter, Planning and control for autonomous excavation. *IEEE Robot. Autom. Lett.* **2**, 2151–2158 (2017).

20. H. Dunlop, D. R. Thompson, D. Wettergreen, Multi-scale features for detection and segmentation of rocks in mars images, in *Proceedings of the IEEE/CVF Conference on Computer Vision and Pattern Recognition* (IEEE, 2007), pp. 1–7.
21. H. Shariati, A. Yeraliyev, B. Terai, S. Tafazoli, M. Ramezani, Towards autonomous mining via intelligent excavators, in *Proceedings of the IEEE/CVF Conference on Computer Vision and Pattern Recognition Workshops* (CVPR, 2019), pp. 26–32.
22. Robot Operating System; https://ros.org.
23. L.-C. Chen, G. Papandreou, I. Kokkinos, K. Murphy, A. L. Yuille, Deeplab: Semantic image segmentation with deep convolutional nets, atrous convolution, and fully connected CRFs. *IEEE Trans. Pattern Anal. Mach. Intell.* **40**, 834–848 (2017).
24. C. Liu, L.-C. Chen, F. Schroff, H. Adam, W. Hua, A. L. Yuille, L. Fei-Fei, Auto-deeplab: Hierarchical neural architecture search for semantic image segmentation, in *Proceedings of the IEEE Conference on Computer Vision and Pattern Recognition* (CVPR, 2019), pp. 82–92.
25. K. He, G. Gkioxari, P. Dollár, R. Girshick, Mask r-cnn, in *Proceedings of the IEEE International Conference on Computer Vision* (2017), pp. 2961–2969.
26. J. Xue, H. Zhang, K. Dana, Deep texture manifold for ground terrain recognition, in *Proceedings of the IEEE/CVF Conference on Computer Vision and Pattern Recognition* (CVPR, 2018).
27. H. Dong, J. Pan, L. Xiang, Z. Hu, X. Zhang, F. Wang, M.-H. Yang, Multi-scale boosted dehazing network with dense feature fusion, in *Proceedings of the IEEE/CVF Conference on Computer Vision and Pattern Recognition* (CVPR, 2020), pp. 2157–2167.
28. Y. Zhang, K. Li, K. Li, L. Wang, B. Zhong, Y. Fu, Image super-resolution using very deep residual channel attention networks, in *Proceedings of European Conference on Computer Vision* (ECCV, 2018), pp. 286–301.
29. J. Zhao, L. Zhang, TaskNet: A neural task planner for autonomous excavator, in *2021 IEEE International Conference on Robotics and Automation* (ICRA, 2021).
30. S. Reed, N. De Freitas, Neural programmer-interpreters. arXiv:1511.06279 [cs.LG] (19 November 2015).
31. M. Kalakrishnan, P. Pastor, L. Righetti, S. Schaal, Learning objective functions for manipulation, in *2013 IEEE International Conference on Robotics and Automation* (IEEE, 2013), pp. 1331–1336.
32. M. Kalakrishnan, S. Chitta, E. Theodorou, P. Pastor, S. Schaal, STOMP: Stochastic trajectory optimization for motion planning, in *2011 IEEE International Conference on Robotics and Automation* (IEEE, 2011), pp. 4569–4574.
33. C. Park, J. Pan, D. Manocha, ITOMP: Incremental trajectory optimization for real-time re-planning in dynamic environments, in *2012 International Conference on Automated Planning and Scheduling (ICAPS)* (AAAI Press, 2012), pp. 207–215.
34. Y. Yang, L. Zhang, X. Cheng, J. Pan, R. Yang, Compact reachability map for excavator motion planning, in *2019 IEEE/RSJ International Conference on Intelligent Robots and Systems* (IROS, 2019), pp. 2308–2313.
35. J. Zhang, S. Singh, Loam: Lidar odometry and mapping in real-time, in *Proceedings of Robotics: Science and Systems* (RSS, 2014).
36. D. Kothandaraman, R. Chandra, D. Manocha, SS-SFDA: Self-supervised source-free domain adaptation for road segmentation in hazardous environments. arXiv:2012.08939 [cs.CV] (27 November 2020).
37. D. Dolgov, S. Thrun, M. Montemerlo, J. Diebel, Path planning for autonomous vehicles in unknown semi-structured environments. *Int. J. Robot. Res.* **29**, 485–501 (2010).
38. C. Berger, B. Rumpe, Engineering autonomous driving software, in *Experience from the DARPA Urban Challenge* (Springer-Verlag, 2012), pp. 243–271.

Acknowledgments: We thank all current and former team members in Robotics and Auto-Driving Lab (RAL) at Baidu Research for contribution and support to this project, including R. Yang, H. Jiang, Y. Yang, Z. Deng, X. Chen, H. Xu, Q. Lu, Z. Ye, Z. He, H. Ding, Q. Guo, J. Fang, and D. Zhou, and our collaborators, including J. Pan. **Funding:** This project was not supported by government funding. **Author contributions:** All authors contributed to the project, including system design, implementation, testing, validation, and paper writing. **Competing interests:** The authors declare that they have no competing interests. **Data and materials availability:** All data needed to evaluate the conclusions in the paper are present in the paper or the Supplementary Materials.

Submitted 14 August 2020
Accepted 7 June 2021
Published 30 June 2021
10.1126/scirobotics.abc3164

Citation: L. Zhang, J. Zhao, P. Long, L. Wang, L. Qian, F. Lu, X. Song, D. Manocha, An autonomous excavator system for material loading tasks. *Sci. Robot.* **6**, eabc3164 (2021).

An autonomous excavator system for material loading tasks

Liangjun Zhang, Jinxin Zhao, Pinxin Long, Liyang Wang, Lingfeng Qian, Feixiang Lu, Xibin Song and Dinesh Manocha

Sci. Robotics **6**, eabc3164.
DOI: 10.1126/scirobotics.abc3164